Attitude Control Configuration for Multi-rotors: A Comparative Study Using Propeller Test-Bench and Wind Tunnel

Binh-Minh Nguyen*a), Member, Hiroshi Fujimoto*, Senior-member

This paper presents a comparative study on attitude control of multi-rotors using propeller test-bench and wind tunnel. Test results show that the traditional single-layer control configuration, which directly outputs pulse-width-modulation commands to motor drives, cannot guarantee good tracking performance under strong disturbance. Instead, it recommended utilizing a hierarchical decentralized control system which controls the attitude in the upper-layer, and propeller speeds in the lower-layer. Especially, the control performance can be further improved by providing disturbance observer to both layers.

Keywords: multi-rotor, propeller, disturbance observer, hierarchical decentralized control, yaw angle control.

1. Introduction

Multi-rotor flying vehicles have been increasingly utilized in many practical applications of human society [1]. Consequently, various motion control approaches have been proposed to stabilize the position and attitude of multi-rotor bodies (body for short from now on) in the three-dimensional Euclidean space. To mention just a few, we have fuzzy logic [2], sliding mode [3], passivity based damping assignment [4], optimal control [5] and nonlinear disturbance observer [6]. Although such controllers are different in their algorithm, they share the same philosophy: Through feedback control of the motion variables of the body, they directly output the pulse-width-modulation commands to the motor drives.

Unfortunately, the above design philosophy, which is solely based on the body dynamics, cannot always maintain the stability and robustness of the total system [7]. This is because the multi-rotor consists of not only the body but also a bunch of propeller actuators. The *local* actuators physically interact with each other to generate the *global* motion of the body. To take into account both global and local dynamics, we recently proposed several strategies based on Circle Popov criterion [7], generalized frequency variable [8]. However, the above studies [7] [8] only utilized the global motion controllers without highlighting the local actuator controllers. This motivated us to perform comparative study on two system configurations as follows:

(i) Single-layer configuration: The control system only consists of the global controller for body motion control.

(ii) Hierarchical decentralized configuration: Together with the upper-layer controller, there are a bunch of local-controllers in the lower-layer for feedback control of propellers' speeds.

Furthermore, it is important to evaluate the different controller candidates under strict operational conditions, such as under strong disturbance and model uncertainties.

Aiming at the aforementioned goals, this paper focuses on attitude control of multi-rotor. A dual-motor propeller test-bench, as shown in Fig. 1, was developed to simultaneously investigate the body's yaw-motion and the propeller's rotational motion. A wind tunnel was used to generate strong disturbance to the system. Several controller candidates and their integration were performed for comparison, including linear quadratic regulator, proportional derivative controller, proportional integral controller, and disturbance observer.

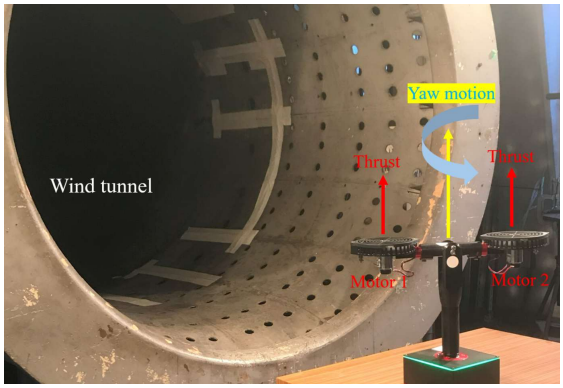

Fig. 1. Dua-motor propeller test-bench under study.

2. Test-bench under study

2.1 Test-bench description Each propeller is driven by a direct current (DC) motor. The motor is provided with a motor drive, which can be utilized to control the motor speed. The motor current and motor speed can be obtained in real time using current sensor and encoder, respectively. By rotating the motor, thrust force is generated at each propeller. This consequently generates a moment that rotates the test-bench about the vertical axis (yaw motion). The system was provided with the other encoders to measure the yaw angle and pitch angle (Note that, although the pitch motion is available, it was locked in this study). The control algorithm can be built using Matlab/Simulink using Quanser control unit [9]. The main specifications and parameters of the test-bench are shown in Table 1. To generate external disturbances, this study utilized a wind tunnel at Hongo Campus, the University of Tokyo. The wind tunnel can blow the wind up to 20 m/s.

a) Correspondence to: Binh-Minh Nguyen.
E-mail: nguyen.binhminh@edu.k.u-tokyo.ac.jp
* The University of Tokyo, Department of Advanced Energy.
5-1-5 Kashiwanoha, Kashiwa, Chiba, Japan 277-8561

Table 1. Test-bench specification.

Thrust displacement	$L = 0.158\ m$
Yaw encoder	4096 counts/revolution
Inertial measurement unit	IIM-42652 6-Axis MEMS
Thrust constant	$\mu = 7.7 \times 10^{-7}\ N.rad^{-2}.s^{-2}$
Speed-to-yaw-moment gain	$S_{gn} = 10 \times 10^{-5} N.m.s.rad^{-1}$
Yaw motion's inertia	$J_{gn} = 0.022\ N.m.s.rad^{-2}$
Yaw motion's damping	$D_{gn} = 0.022\ N.m.s.rad^{-1}$
Motor's amplification gain	$K_n = 19.0\ rad.s^{-1}.V^{-1}$
Motor's time constant	$T_n = 0.165\ s$

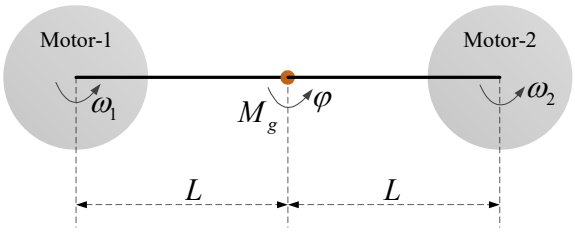

Fig. 2. Half-quadrotor model of yaw motion.

2.1 System modeling By linearizing the thrust characteristics, the yaw moment M_g acting on the test-bench can be approximated as a linear function of the propeller speeds ω_i:

$$M_g = S_{gn}\omega_1 + S_{gn}\omega_2 \quad \cdots\cdots (1)$$

where S_{gn} can be obtained via parameter identification using experimental data. To represent the global dynamics, the transfer functions from the yaw moment to the yaw rate v_φ and yaw angle φ are expressed as follows, respectively:

$$P_{gn}^{v\varphi}(s) = \frac{1}{J_{gn}s + D_{gn}}, P_{gn}^{\varphi}(s) = \frac{1}{(J_{gn}s + D_{gn})s} \quad \cdots\cdots (2)$$

To represent the local dynamics, the transfer function from the motor voltage to the propeller speed is normalized as follows:

$$P_{ln}(s) = \frac{K_n}{T_n s + 1} \quad \cdots\cdots (3)$$

3. Problem setting

3.1 System configurations This study compares two control configurations, namely "single-layer" and "hierarchical decentralized," as shown in Figs. 3a and 3b, respectively. In Fig. 3a, C_g is a global controller that tracks the real yaw angle with the reference value φ^*. This controller outputs the desired value of yaw moment M_g^*. This signal is transformed to the voltage commands $V_{1,2}^*$ by using the moment-to-voltage (M2V) operator. This is the basic control configuration which has been utilized in many existing methods in literature [1] ~ [8]. Unlike this basic configuration, Fig. 3b demonstrates a new control configuration with two layers. The upper-layer is provided with the global controller and a moment-to-speed (M2S) operator, which transforms the desired yaw moment to the reference values $\omega_{1,2}^*$ of the propeller speeds. In the lower-layer, the local controller C_l is to control the propeller speed to generate the voltage commands of the motor drivers.

3.2 Control methods for comparison Using the aforementioned configurations, four methods were performed for comparison, and they are summarized as in Table 2.

Method 1 (Global LQR): From (2), the following state space equation is established:

$$\dot{X} = AX + BU \quad \cdots\cdots (4)$$

where $X = \begin{bmatrix} v_\varphi \\ \varphi \end{bmatrix}, U = M_g, A = \begin{bmatrix} \frac{-D_{gn}}{J_{gn}} & 0 \\ 1 & 0 \end{bmatrix}, B = \begin{bmatrix} \frac{1}{J_{gn}} \\ 0 \end{bmatrix}$

The LQR's feedback gains are obtained by solving a quadratic cost function with a symmetric positive semidefinite matrix Q to penalize the transient state deviation, and a strictly symmetric positive definite matrix R to penalize the control effort [5]. In this study, we selected $Q = diag\{75, 0.1\}$ and $R = 0.01$.

Method 2 (Global PD-DOB): The upper-layer consists of a PD controller and a DOB [10]. The controllers can be designed using a robust control problem setting shown in Fig. 4, where the tracking controller and the low-pass filter of the disturbance observer are respectively expressed as:

$$C_{g,pd}(s) = K_{p,g} + \frac{K_{d,g}s}{\tau_g s + 1} \quad \cdots\cdots (5)$$

$$Q_g(s) = \frac{K_{dob,g}}{\tau_{dob,g}s + 1} \quad \cdots\cdots (6)$$

where τ_g and $\tau_{dob,g}$ are the time-constants, and Δ_g represents the multiplicative perturbation of the yaw motion. It is assumed that the infinity norm of Δ_g is 0.1. Consequently, the control gains were obtained using a μ-synthesis design procedure [11].

Method 3 (Global PD-DOB, Local PI): The upper-layer of **Method 3** is designed with a PD controller and a DOB. In addition, a PI is used to control the propeller speed in the lower-layer.

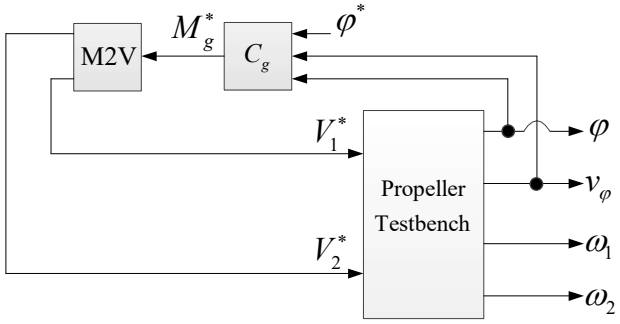

(a) Single-layer configuration.

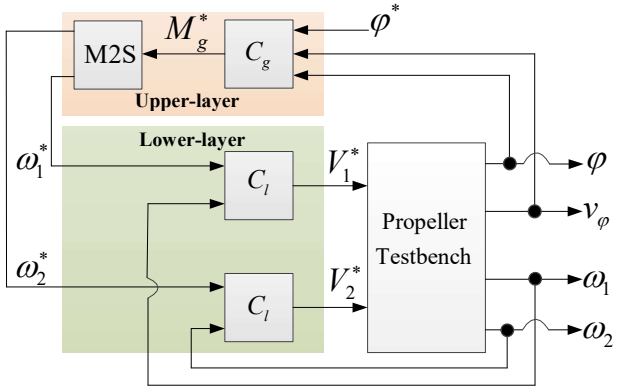

(b) Hierarchical decentralized configuration.

Fig. 3. Two control configurations.

Table 2. Summary of the comparative study.

Method No.	Configuration	Description	Ref. No.
1	Single-layer	C_g is a linear quadratic regulator (LQR)	(5)
2	Single-layer	C_g consists of a proportional derivative (PD) controller with a disturbance observer (DOB)	(10)
3	Hierarchical decentralized	C_g consists of a PD controller and a DOB, and C_l is a proportional integral (PI) controller	(12)
4	Hierarchical decentralized	C_g consists of a PD controller and a DOB, and C_l consists of a PI controller and a DOB	(12)

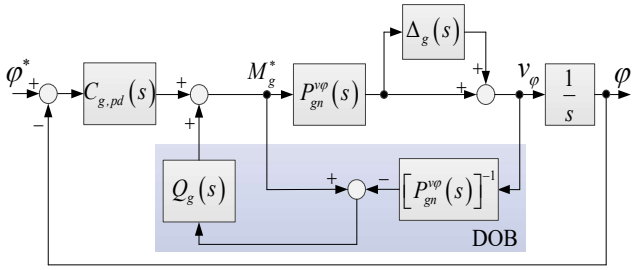

Fig. 4. Robust problem setting for **Method 2**.

Method 4 (Global PD-DOB, Local PI-DOB): The upper-layer of **Method 4** is the same as that of **Method 3**. On the other hand, the lower-layer **Method 4** consists of a PI controller and a DOB. The transfer functions of the PI and the DOB's low-pass filter are respectively expressed as:

$$C_{l,pi}(s) = K_{p,l} + \frac{K_{i,l}}{s} \quad \text{..... (7)}$$

$$Q_l(s) = \frac{K_{dob,l}}{\tau_{dob,l}s + 1} \quad \text{..... (8)}$$

The general robust control problem setting in Fig. 5 was utilized to design the controllers for **Methods 3** and **4**. Here, **G** and **L** are the block of the upper-layer and lower-layer dynamics, respectively. In the upper-block, y_g^* is the reference value, such as the reference yaw angle in this study. We define the matrix $\Delta_l = diag\{\Delta_{l,1}, \Delta_{l,2}\}$ represents the perturbations of the local actuator dynamics (3). The operator **A** represents the aggregation from lower-layer to upper-layer dynamics as shown in (1). On the other hand, the operator **D** represents the distribution of the propeller speed references from upper-layer to lower-layer. The global and local disturbances are denoted by the scalar d_g and vector $\mathbf{d}_l$, respectively. The performance of the upper-layer and lower-layer can be treated as the sensitivities from d_g to y_g and $\mathbf{d}_l$ to $\mathbf{y}_l$, respectively.

Recently, we have developed a procedure to analyze the control performances and design the controllers using a nominal model set to be shared between two control layers [12]. Using the proposed method [12], a selection of the controllers that compromise the trade-off between the lower-layer and upper-layer can be given as

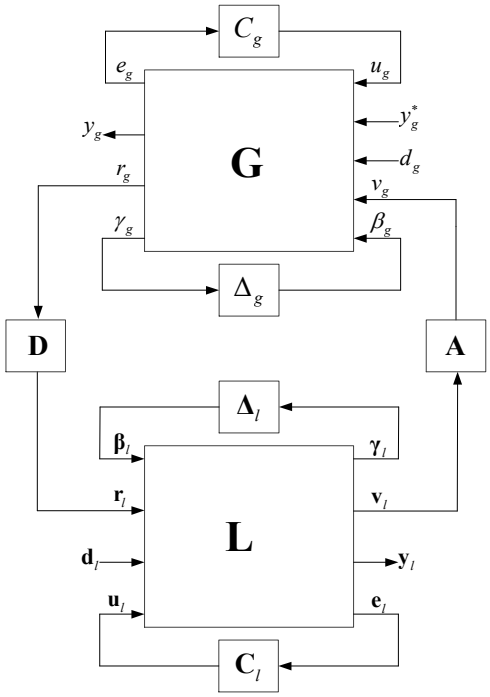

Fig. 5. HD-DOBC in global/local framework.

follows:

$$\text{Lower: } C_{l,pi}(s) = 0.1645 + \frac{1.3569}{s},\ Q_l(s) = \frac{0.9}{0.05s + 1}$$

$$\text{Upper: } C_{g,pd}(s) = 59.5260 + \frac{2.3451s}{0.0133s + 1},\ Q_g(s) = \frac{0.8}{0.08s + 1}$$

4. Experimental results

Test-bench experiment of four methods in Table 2 were conducted under the wind speed of 10 m/s, which is the wind speed number five in the Beaufort scale. In addition, a software disturbance was introduced to the voltage command of the motor driver at 20 seconds.

As shown in Fig. 6, the yaw tracking performance of **Method 1** was very bad. This is due to the fact that **Method 1** is merely an

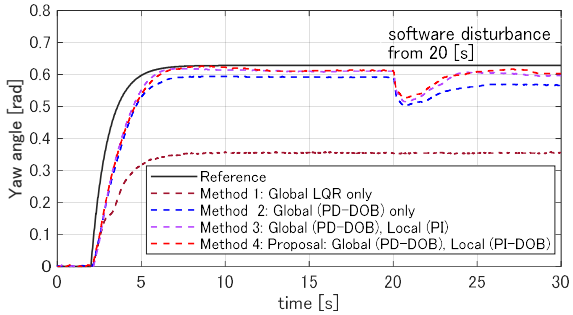

(a) Overall results.

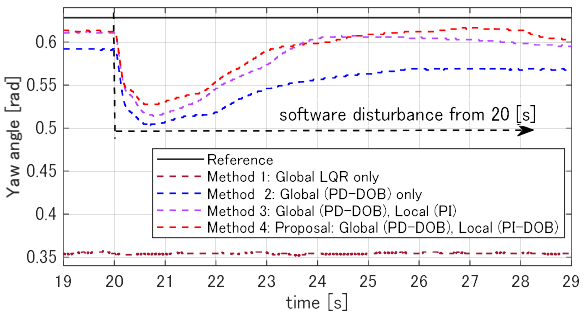

(b) Response to software disturbance.

Fig. 6. Yaw angle control under strong disturbance.

LQR without disturbance observer. Thus, it cannot compensate for both disturbances and model uncertainties in the body dynamics and actuator dynamics.

Method 2 also belongs to the single-layer group. Thanks to the disturbance observer, it attained much better control performance in comparison to **Method 1**. However, the gap between the real and reference yaw angle is still noticeable.

By combining the upper-layer and lower-layer controllers, **Method 3** successfully enhanced the yaw tracking performance in comparison with **Methods 1 and 2**. This improvement can be explained as follows: To maintain a good yaw angle tracking performance, it is essential for the local propellers to generate the yaw moment that matches with the desired yaw moment from the global controller. The yaw moment, however, is generated by the rotational motions of the propellers. Without propeller speed controllers, the rotational motions of the propellers might be easily deteriorated, especially when the multirotor operates under strong disturbance conditions.

Finally, **Method 4** was provided with disturbance observer in both control layers. It reaches the best control performance among the four candidates in Table 1. Root-mean-square-error (RMSE) of the four methods were calculated and demonstrated in Fig. 7. Transparently, **Method 4** reduces the RMSE by 33% and 5% compared with those of **Method 2** and **Method 3**, respectively.

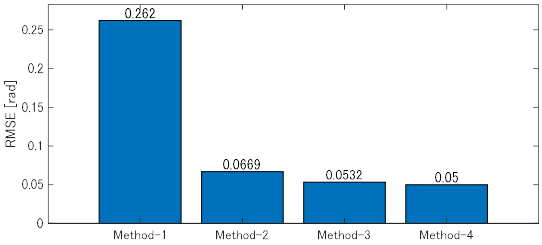

Fig. 7. RMSEs of yaw angle tracking error.

5. Conclusions

The comparative study in this paper clarifies that the hierarchical decentralized control configuration would be selected for future multi-rotor motion control. Especially, the control performance can be further improved by implementing disturbance observers for both body control layer and actuator control layer. In future, we will investigate other candidates of the controllers for the hierarchical decentralized configuration. As this paper only focuses on yaw angle control, future study will extend the hierarchical decentralized configuration to cover other motion control objectives. Furthermore, we will develop control theories and design procedures to analyze the hierarchical decentralized configuration of multiple objectives.

Acknowledgement

This research was supported in part by the Kakenhi Project 22K14283 and the Nagamori Grant for young researchers.

References

(1) S. Wandelt, S. Wang, C. Zheng, and X. Sun: "AERIAL: A Meta Review and Discussion of Challenges Toward Unmanned Aerial Vehicle Operations in Logistics, Mobility, and Monitoring", IEEE Transactions on Intelligent Transportation Systems, Vol. 25, Iss. 7, pp. 6276-6289 (2024).

(2) A. Al-Mahturi, F. Santoso, M. A. Garratt, and S. G. Anavatti: "Self-Learning in Arieal Robotics Using Type-2 Fuzzy Systems: Case Study in Hovering Quadcopter Flight Control," IEEE Access, Vol. 9, pp. 119520-119532 (2021).

(3) J. Zhao, Z. Xie, M. Xiao, F. Xu, and Z. Gao: "A Sliding Mode Control Algorithm Based on Improved Super-Twisting and Its Applications to Quadrotors," Journal of Control and Decisions, Vol. 10, Iss. 3, pp. 433-442 (2022).

(4) M. E. Guerrero-Sánchez, D. A. Mercado-Ravell, R. Lozano, and C. D. García-Beltrán: "Swing-attenuation for a Quadrotor Transporting a Cable-suspended Payload," ISA Transactions, Vol. 68, pp. 433-449 (2017).

(5) M. R. Cohen, K. Abdulrahim, and J. R. Forbes: "Finite-Horizon LQR Control of Quadrotors on SE2(3)," IEEE Robotics and Automation Letters, Vol. 5, No. 4, pp. 5748-5755 (2020).

(6) M. Sharma and I. Kar: "Nonlinear Disturbance Observer Based Geometric Control of Quadrotors," Asian Journal of Control, Vol. 23, No. 4, pp. 1936-1951 (2021).

(7) B.-M. Nguyen, T. Kobayashi, K. Sekitani, M. Kawanishi, and T. Narikiyo: "Altitude Control of Quadcopters with Absolute Stability Analysis," IEEJ Journal of Industry Applications, Vol. 11, No. 4, pp. 562-572 (2022).

(8) B.-M. Nguyen, S. Hara, V. P. Tran: "A Multi-Agent Approach to Landing Speed Control with Angular Rate Stabilization for Multirotors," IEEE Vehicle Power and Propulsion Conference, pp. 1-6 (2022).

(9) B.-M. Nguyen, S. Nagai, and H. Fujimoto: "Multirate Attitude Control of Dual-Rotor System Considering Propeller Loss of Effectiveness," 49th Annual Conference of the IEEE Industrial Electronics Society (2023).

(10) X. Lyu, J. Zhou, H. Gu, Z. Li, S. Shen and F. Zhang: "Disturbance Observer Based Hovering Control of Quadrotor Tail-Sitter VTOL UAVs Using H∞ Synthesis," IEEE Robotics and Automation Letters, Vol. 3, No. 4, pp. 2910-2917 (2018).

(11) K. Zhou and J. C. Doyle: "Essentials of Robust Control," Prentice-Hall (1998).

(12) B.-M. Nguyen, S. Hara, and H. Fujimoto: "Disturbance Observer-Based Global/Local Control Using Shared Model Set: Design Concept with Practical Applications to Multi-rotors," IEEJ Journals of Industry Applications, Vol. 14, No. 3 (2025, to be published).